

# *Least Squares Optimisation Algorithm Based System Identification of an Autonomous Underwater Vehicle*

*Nhận dạng hệ thống cho phương tiện ngầm tự hành*

*sử dụng thuật toán tối ưu bình phương cực tiểu*

Minh Q. Tran<sup>a,\*</sup>, Supun A. T. Randeni P.<sup>a</sup>, Hung D. Nguyen<sup>a</sup>, Jonathan Binns<sup>a</sup>,  
Shuhong Chai<sup>a</sup> and Alexander L. Forrest<sup>a,b</sup>

<sup>a</sup>Australian Maritime College, University of Tasmania, Launceston, Australia

<sup>b</sup>University of California – David, Incline Village, NV, USA

\*e-Mail: [Quang.Tran@utas.edu.au](mailto:Quang.Tran@utas.edu.au)

## Abstract

This paper presents the identification of mathematical models governing dynamics in both the vertical and horizontal planes for a axisymmetric, torpedo-shaped *Gavia* class Autonomous Underwater Vehicle (AUV), based on a least squares optimisation algorithm. Rather than using the least squares algorithm to roughly estimate the mathematical models in a fixed time period, a simulator is developed based on least squares optimisation algorithm with the goal of accurately predicting the system response over time starting from initial conditions. The general equations for six degrees of freedom motions are decoupled into non-interacting longitudinal and lateral subsystems in the form of linear state space models with unknown parameters. These unknown parameters are initially determined by applying a least squares algorithm for experimental data collected from the AUV's on-board sensors. The previously identified models are then optimised to form the simulator able to estimate the system response. The numerically simulated data from the simulator show a good agreement with the field measured data. The simulator provides a useful tool to examine the manoeuvrability of AUV. The verification process proved that the least squares algorithm could be utilised as an optimisation algorithm in the system identification of autonomous underwater vehicle.

**Keywords:** Autonomous Underwater Vehicle, System Identification, Least Squares Optimisation Algorithm, State Space model.

## Tóm tắt

Bài báo trình bày về nhận dạng hệ thống của mô hình toán biểu diễn động lực học trong mặt phẳng thẳng đứng và ngang cho phương tiện ngầm tự hành (AUV) *Gavia* có hình dạng thủy lôi đối xứng, dựa trên thuật toán tối ưu bình phương cực tiểu. Không chỉ sử dụng thuật toán bình phương cực tiểu để ước đoán tổng quan mô hình toán học trong một khoảng thời gian nhất định, một chương trình mô phỏng được phát triển với mục tiêu dự đoán chính xác đáp ứng của hệ thống

từ những dữ kiện ban đầu nhất định. Phương trình tổng quát mô tả chuyển động sáu bậc tự do được phân tách thành những hệ con riêng biệt trong mặt phẳng ngang và thẳng đứng dưới dạng mô hình không gian trạng thái chứa các tham số. Các tham số này ban đầu được xác định bằng cách áp dụng thuật toán bình phương cực tiểu cho dữ liệu thực nghiệm thu thập trực tiếp từ những cảm biến trên AUV. Mô hình này sau khi được xác định sẽ được tiếp tục tối ưu hóa để tạo thành chương trình mô phỏng dự đoán đáp ứng của phương tiện. Dữ liệu mô phỏng số từ chương trình mô phỏng cho kết quả phù hợp với dữ liệu thu thập từ thực nghiệm. Chương trình mô phỏng sẽ hỗ trợ đặc lực cho việc nghiên cứu chuyển động của AUV. Quá trình kiểm chứng đã cho thấy thuật toán tối ưu bình phương cực tiểu có thể được ứng dụng trong quá trình nhận dạng hệ thống của phương tiện ngầm tự hành.

**Từ khóa:** Phương tiện ngầm tự hành, Nhận dạng hệ thống, Thuật toán tối ưu bình phương cực tiểu, Mô hình không gian trạng thái.

## Nomenclature

Symbol	Description
$\mathbf{f}$	vector of hydrodynamic forces and moments
$\mathbf{g}$	vector of buoyancy, gravitational, hydrostatic forces and moments
$\mathbf{M}$	body inertial matrix including hydrodynamic added masses
$\mathbf{J}$	Euler angle transformation matrix
$\boldsymbol{\eta}$	position and orientation vector in the Earth-fixed frame
$\mathbf{v}$	state vector in body-fixed frame
$\boldsymbol{\theta}$	unknown coefficients vector

## Abbreviations

AMC	Australian Maritime College
AUV	Autonomous Underwater Vehicle
CFD	Computational Fluid Dynamic
DOF	Degree of freedom
EFD	Experimental Fluid Dynamic
INS	Inertial Navigation System

LS	Least Squares
ROV	Remote Operated Vehicle
SI	System Identification

## 1. Introduction

The recent development in the applications of Autonomous Underwater Vehicles (AUVs) require conventional torpedo shaped AUVs to be capable of accomplishing missions of various complexity in challenging operational environments; for example, under ice explorations, deep-ocean floor surveys and industrial subsea infrastructure inspections [1, 2]. Besides emerging modern control system designs, configuration modifications and battery life improvements, new propulsion system designs are of great interest to facilitate new applications. The National Centre for Maritime Engineering and Hydrodynamics at Australian Maritime College (AMC), University of Tasmania has been validating a new type of propulsion unit named a Cyclic and Collective Pitch Propeller (CCPP) aiming to improve the AUV overall performance for complex mission tasks. The overall performance of an AUV equipped with the CCPP propulsion unit compared to that of a conventional propulsion system is to be evaluated using a numerical study, choosing the *Gavia* class AUV at AMC as the research platform. With a long term objective of assessing the high-fidelity simulation of AUV with different propulsion configuration, this work develops a system identification (SI) approach in order to accurately and rapidly identify the mathematical model of the AUV. There are four fundamental approaches to determine a mathematical model of an underwater vehicle. The first method is a theoretical approach to calculate the coefficients by using empirical equations and component build-up method [3]. The second is using Experimental Fluid Dynamic (EFD) methods such as captive model experiments [4]. The third method is conducting Computational Fluid Dynamic (CFD) simulations to replicate the EFD testings [5, 6] and the final method is System Identification (SI). Using this last method, the hydrodynamic coefficients that characterise the vehicle dynamics of an AUV are estimated using data acquired by on-board sensors from free running field trials [7].

The theoretical, EFD and CFD approaches are generally used in the preliminary design stage to estimate hydrodynamic coefficients of potential AUV. In contrast, an SI method can be effectively used to determine the parameters of a fully developed vehicle. This approach provides a dynamic model with a high degree of fidelity since the experimental data utilised for modelling are acquired under real operational conditions. Also, the variation of the hydrodynamic coefficients due to changes in the external configuration of a modular underwater vehicle (for example, in the case of adding an extra payload module to the base vehicle configuration of the vehicle) can be quickly and cost effectively determined using SI. However, there are some practical concerns associated with performing SI on AUVs. The first is that the experimental data were collected in the presence of noise and turbulence. The

noise could result in an increased variance in the least squares parameter estimation. Therefore the SI approach requires the physical system to be sufficiently instrumented in order to accurately measure the necessary state variables with minimum noise effects. The second issue is that the estimation of the mathematical model relied on the data collected from close-loop feedback control system which may cause noise to be correlated to the input [8].

A wide range of SI algorithms including Least Squares (LS), Extended Kalman filter (EKF), Maximum Likelihood (ML) and Neural Network (NN) have been developed over the past years [8]. These methods generally minimise the errors between vehicle state variables predicted by the dynamic model and actual measured state variables. Since the underwater vehicle dynamic equations of motion can be expressed in state space models linearized in the range of the cruising conditions, the LS algorithm becomes a favourable approach for practical system identification which can be derived in both the offline condition (Ordinary or Weighted Least Squares) and online condition (Recursive Least Squares).

While there has been significant literature on LS technique for open frame Remote Operated Vehicles (ROVs) [7, 9, 10], studies for torpedo-shaped AUVs are limited. These AUV based studies are generally carried out in the horizontal plane for lateral subsystem [11, 12] or the vertical plane for longitudinal subsystem respectively [13]. This study utilises the offline LS method to derive an experimentally validated state space model that is able to describe the manoeuvring characteristics of a torpedo shaped AUV for both steering and diving subsystems. Instead of predicting system response based on given current states as in previous works, the simulator resulted from the proposed procedure derives the response from specific initial conditions to meet the desired requirements.

The paper is structured as follows: Section II derives the simplified mathematical model for motion of the AUV in both horizontal and vertical planes. Section III outlines the proposed identification procedure and least squares method. Summary of experimental setup and data processing is described in Section IV. Section V presents the identification results and verification. Finally overall discussion and future works are summarised in Section VI.

## 2. Mathematical model of the AUV

### 2.1 *Gavia* AUV configuration overview

A *Gavia* class modular, torpedo-shaped AUV was used for the investigation. The vehicle in its tested configuration consisted of a Nose Cone Module, Battery Module, Module, Acoustic Doppler Current Profiler (ADCP) Module, Inertial Navigation System (INS) Module, Control Module and a Propulsion Module. There are some transducers equipped with AUV such as Obstacle avoidance sonar, Acoustic modem transducer and side scan sonar transducer.

The overall length of the vehicle was 2.7 m and a maximum hull diameter of 0.2 m and the dry weight in air was approximately 70 kg . The configuration of *Gavia* AUV is illustrated in Fig. 1.



Fig. 1. *Gavia* Autonomous Underwater Vehicle [14]

The AUV is propelled and manoeuvred with a three-bladed propeller and four independent control surfaces in an “X-wing” configuration located aft of the propeller. The control surfaces can be commanded separately by independent servo motors and are employed simultaneously to generate accurate forces and moments. The whole unit is protected inside a Kort nozzle. This propulsion configuration is unique to Teledyne *Gavia* and provides high efficiency for both low speed and high speed manoeuvres. The pictures of propulsion system are given in Fig. 2.

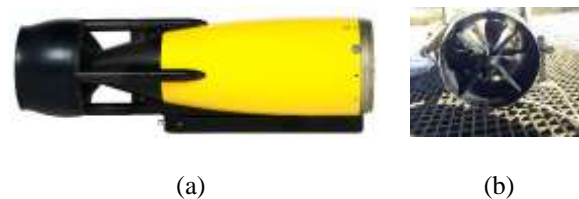


Fig. 2. *Gavia* Propulsion system. (a) Side View of the Propulsion Module. (b) The Control Surfaces in “X-wing” configuration

### 2.2 Equations of dynamic motion of the AUV

The general mathematical model of a marine vehicle was chosen to represent the relationship between inputs and outputs of a system. Two reference frames used to describe the motion of the *Gavia* AUV are shown in Fig. 3.

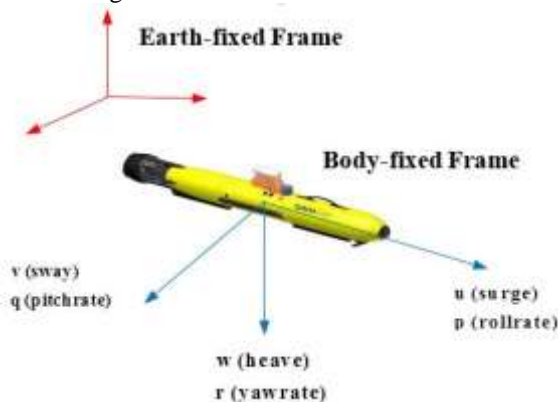


Fig. 3. Reference frames of *Gavia* AUV model

*A priori* knowledge about the system can be used to select an appropriate model [16]. The underwater vehicle is regarded as a rigid body in three-

dimensional space. The six-degree-of-freedom (6-DOF) in an irrotational, inviscid, uniform and constant density fluid can be expressed by the differential equation of motion given in equation (1) [17, 18]:

$$\mathbf{M}(\mathbf{v}, \boldsymbol{\theta}, t) \dot{\mathbf{v}} = \mathbf{g}(\mathbf{v}, \boldsymbol{\theta}, t) + \mathbf{f}(\mathbf{v}, \boldsymbol{\theta}, t) + \boldsymbol{\tau}(t) \quad (1)$$

where

$\mathbf{v}(t) \in \mathbb{R}^6$ : the state vector expressed in Body-fixed frame, generally constituted by linear and angular velocities,  $\mathbf{v} = [u \ v \ w \ p \ q \ r]^T$

$\boldsymbol{\theta}$ : the unknown coefficients vector, including hydrodynamic derivatives and inertial coefficients

$\mathbf{M}(\mathbf{v}, \boldsymbol{\theta}, t) \in \mathbb{R}^{6 \times 6}$ : the body inertial matrix including hydrodynamic added masses

$\mathbf{g}(\mathbf{v}, \boldsymbol{\theta}, t) \in \mathbb{R}^6$ : the vector of buoyancy, gravitational, hydrostatic forces and moments

$\mathbf{f}(\mathbf{v}, \boldsymbol{\theta}, t) \in \mathbb{R}^6$ : the vector of hydrodynamic forces and moments (damping forces)

$\boldsymbol{\tau}(t) \in \mathbb{R}^6$ : the vector of control forces and moments

The vehicle kinematic equations are expressed as:

$$\dot{\boldsymbol{\eta}} = \mathbf{J}(\boldsymbol{\eta}) \mathbf{v} \quad (2)$$

where

$\mathbf{J}(\boldsymbol{\eta})$ : an Euler angle transformation matrix

$\boldsymbol{\eta} = (x \ y \ z \ f \ q \ y)^T$ : position and orientation vector expressed in the Earth-fixed frame

### 2.3 Assumptions and simplified dynamic model

There are a large number of linear as well as nonlinear hydrodynamic derivatives presented in the 6-DOF mathematical model of the AUV. A widely used approximation can be achieved if it is assumed that  $\mathbf{f}(\mathbf{v}, \boldsymbol{\theta}, t)$  consists of linear drag forces only,  $\mathbf{g}(\mathbf{v}, \boldsymbol{\theta}, t)$

consists of buoyancy forces only and if the inertia matrix including added mass is time-space invariant and diagonal [19]. This approximation is proved to be reasonable through simulation of identified models.

The complete 6-DOF can be decomposed into three essentially non-interacting subsystems to describe the hydrodynamics of an AUV: (a) the lateral subsystem, (b) the longitudinal subsystem and (c) the speed subsystem. This traditional approach is applicable in practice for streamlined torpedo-shaped AUVs when the coupling between subsystems is weak and may be reasonably neglected without serious loss of information [12, 20]. In this work, the lateral subsystem and longitudinal subsystem are of specific interest, the vehicle is controlled at constant forward speed. The speed subsystem considering the modelling of propeller by using EFD will be discussed in other study.

The additional assumptions in the horizontal (x-y plane) and vertical planes (x-z plane) for decoupled

Table 1. Assumptions in horizontal and vertical planes

Horizontal plane (lateral subsystem)	Vertical plane (Diving subsystem)
Heave velocity $w = 0$	Sway velocity $v = 0$
Roll angle $\phi = 0$	Roll angle $\phi = 0$
Pitch angle $\theta = \text{constant}$ , $\dot{\theta} = 0$	Yaw angle $\psi = \text{constant}$ , $\dot{\psi} = 0$
For small roll and pitch angles, $\dot{\psi} = \frac{\sin \theta}{\cos \theta} q + \frac{\cos \phi}{\cos \theta} r \approx r$	For small pitch angle, $\dot{\theta} = q$

Finally, under the assumption of constant forward speed  $u \gg U_0$ , a corresponding set of linearized time-invariant models are derived in horizontal plane and The lateral subsystem:

vertical plane respectively are presented as follows [15]:

$$\begin{bmatrix} \dot{z} \\ \dot{y} \\ \dot{\phi} \\ \dot{\theta} \end{bmatrix} - \begin{bmatrix} N_{\dot{z}} & 0 \\ 0 & 1 \\ 0 & 0 \\ 0 & 0 \end{bmatrix} \begin{bmatrix} z \\ y \\ \phi \\ \theta \end{bmatrix} + \begin{bmatrix} N_r & 0 \\ N_{\dot{y}} & -1 \\ 0 & 0 \\ 0 & 0 \end{bmatrix} \begin{bmatrix} \dot{z} \\ \dot{y} \\ \dot{\phi} \\ \dot{\theta} \end{bmatrix} + \begin{bmatrix} \dot{N}_{d1} & \dot{N}_{d2} & \dot{N}_{d3} & \dot{N}_{d4} \\ 0 & 0 & 0 & 0 \\ 0 & 0 & 0 & 0 \\ 0 & 0 & 0 & 0 \end{bmatrix} \begin{bmatrix} z \\ y \\ \phi \\ \theta \end{bmatrix} \quad (3)$$

The longitudinal subsystem:

$$\begin{bmatrix} \dot{z} \\ \dot{y} \\ \dot{\phi} \\ \dot{\theta} \end{bmatrix} - \begin{bmatrix} M_{\dot{z}} & 0 \\ 0 & 1 \\ 0 & 0 \\ 0 & 0 \end{bmatrix} \begin{bmatrix} z \\ y \\ \phi \\ \theta \end{bmatrix} + \begin{bmatrix} M_q & \overline{BG_z}W \\ 0 & 0 \\ 0 & U_0 \\ 0 & 0 \end{bmatrix} \begin{bmatrix} \dot{z} \\ \dot{y} \\ \dot{\phi} \\ \dot{\theta} \end{bmatrix} + \begin{bmatrix} M_{d1} & M_{d2} & M_{d3} & M_{d4} \\ 0 & 0 & 0 & 0 \\ 0 & 0 & 0 & 0 \\ 0 & 0 & 0 & 0 \end{bmatrix} \begin{bmatrix} z \\ y \\ \phi \\ \theta \end{bmatrix} \quad (4)$$

where

$I_{yy}, I_{zz}$ : the moment of inertia

$\overline{BG_z}$ : the distance between the centre of gravity and the centre of buoyancy

$N_{\dot{z}}, N_r, N_{\dot{y}}, M_{\dot{z}}, M_q, M_{d1}, M_{d2}, M_{d3}, M_{d4}$ : hydrodynamic coefficients.

They are the partial derivatives of forces and moments with respect to corresponding accelerations, velocities or control surface deflection, e.g.  $N_r = \frac{\partial N}{\partial r}$

Equations (3) and (4) are presented in state space model for computational convenience below:

$$\begin{bmatrix} \dot{z} \\ \dot{y} \\ \dot{\phi} \\ \dot{\theta} \end{bmatrix} = \begin{bmatrix} a_1 & 0 \\ 0 & 1 \\ 0 & 0 \\ 0 & 0 \end{bmatrix} \begin{bmatrix} z \\ y \\ \phi \\ \theta \end{bmatrix} + \begin{bmatrix} b_1 & b_2 & b_3 & b_4 \\ 0 & 0 & 0 & 0 \\ 0 & 0 & 0 & 0 \\ 0 & 0 & 0 & 0 \end{bmatrix} \begin{bmatrix} \dot{z} \\ \dot{y} \\ \dot{\phi} \\ \dot{\theta} \end{bmatrix} \quad (5)$$

where

$$a_1 = \frac{N_r}{I_{zz} - N_{\dot{z}}}$$

$$\begin{bmatrix} \dot{z} \\ \dot{y} \\ \dot{\phi} \\ \dot{\theta} \end{bmatrix} = \begin{bmatrix} c_1 & 0 \\ 0 & 1 \\ 0 & 0 \\ 0 & 0 \end{bmatrix} \begin{bmatrix} z \\ y \\ \phi \\ \theta \end{bmatrix} + \begin{bmatrix} d_1 & d_2 & d_3 & d_4 \\ 0 & 0 & 0 & 0 \\ 0 & 0 & 0 & 0 \\ 0 & 0 & 0 & 0 \end{bmatrix} \begin{bmatrix} \dot{z} \\ \dot{y} \\ \dot{\phi} \\ \dot{\theta} \end{bmatrix} \quad (6)$$

where

$$c_1 = \frac{M_q}{I_{yy} - M_{\dot{\phi}}}, \quad c_2 = -\frac{\overline{BG_z}W}{I_{yy} - M_{\dot{\phi}}}, \quad d_i = \frac{M_{di}}{I_{yy} - M_{\dot{\phi}}}$$

Rewriting equation (5) and (6) with the main focus on equations including parameters needed to be estimated:

$$\dot{\mathbf{x}} = \mathbf{H}_1 \boldsymbol{\theta}_1 \quad (7)$$

$$\dot{\mathbf{x}} = \mathbf{H}_2 \boldsymbol{\theta}_2 \quad (8)$$

where

$$\mathbf{H}_1 = [r \quad d_1 \quad d_2 \quad d_3 \quad d_4]$$

$$\mathbf{H}_2 = [q \quad q \quad d_1 \quad d_2 \quad d_3 \quad d_4]$$

$$\boldsymbol{\theta}_1 = [a_1 \quad b_1 \quad b_2 \quad b_3 \quad b_4]^T$$

$$\boldsymbol{\theta}_2 = [c_1 \quad c_2 \quad d_1 \quad d_2 \quad d_3 \quad d_4]^T$$

Due to *Gavia*'s unique control surface configuration, input signals consist of four independent values  $d_i$  in degrees respectively. In other works [12, 13], there is only one input signal for each subsystem; i.e., elevator input signal for diving subsystem and rudder input signal for steering subsystem. In the state space equations in both steering and diving subsystems,  $a_i, b_i, c_i, d_i$  are the model parameters which consist of physical parameters and hydrodynamic coefficients sufficiently describing the system characteristics. It is

important to note that the hydrodynamic coefficients are not determined specifically but this does not impact the applicability of the identified model. The following section describes the identification procedure and the least squares algorithm implemented to identify  $a_i, b_i, c_i, d_i$ .

### 3. Identification procedure and least squares optimisation algorithm

#### 3.1 Proposed identification procedure

Fig. 4 outlines the critical stages of the utilised system identification procedure based on reference from [22].

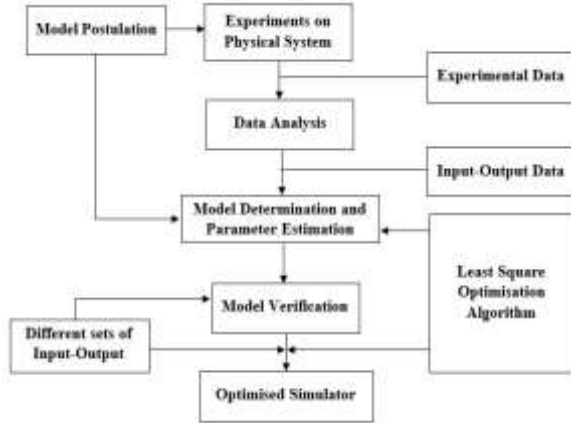


Fig.4. Summary of identification procedure

Within the previous section, the mathematical model of the AUV was developed using a *a priori* model postulation about hydrodynamic characteristics of underwater vehicles. Field experiments were then carried out with a *Gavia* class AUV and the collected data were analysed for parameter estimation. In this stage, the least squares algorithm was utilised to identify the estimated parameters for the previously developed mathematical model. The goal is to find a set of parameter  $\theta_i$  that minimises the average residual error [23]:

$$r_i = \left. \frac{d}{dt} \mathbf{X}_i \right|_{\text{measurement}} - \left. \frac{d}{dt} \mathbf{X}_i \right|_{\text{prediction}} \quad (9)$$

where

$$\mathbf{X}_1 = r, \theta_1 = [a_1 \ b_1 \ b_2 \ b_3 \ b_4]^T \text{ in equation (7)}$$

$$\mathbf{X}_2 = q, \theta_2 = [c_1 \ c_2 \ d_1 \ d_2 \ d_3 \ d_4]^T \text{ in equation (8)}$$

A model verification stage was also executed for different sets of data to verify the identified model. Up to this stage, the identified model was only able to predict the system response ( $r, q$ ) from given current measured states ( $r, q, q$ ) for a certain period of time.

As the principal goal of the study is the desired simulator which could capture the accurate response of vehicle from simulation, the next optimisation process is considered to figure out an updated set of

parameter  $\theta_i$  that minimise the error  $e_i$  between the measured output signal and simulated output signal computed by simulating the identified model from specified initial condition with similar control input signals:

$$e_i = \mathbf{X}_i \Big|_{\text{measurement}} - \mathbf{X}_i \Big|_{\text{simulation}} \quad (10)$$

where  $\mathbf{X}_i \Big|_{\text{simulation}}$  is obtained by simulating equation (7) and (8) with initial set of parameter  $\theta_i$ .

The final results are updated values of parameter  $\theta_i$ . Both minimisation processes for equation (9) and (10) are based on the least squares algorithm which is presented in the following part.

#### 3.2 Least Squares Optimisation algorithm

The dynamic equations (7) and (8) can be written in the form of equation (11)

$$\mathbf{y} = \mathbf{H}\theta \quad (11)$$

where

$\mathbf{H}$  : the measured state and control input vector  
 $\mathbf{y}$  : the estimated output vector

The measured output vector  $\mathbf{z}$  of  $\mathbf{y}$  is defined

$$\mathbf{z} = \mathbf{H}\theta + \boldsymbol{\varepsilon} \quad (12)$$

where

$\boldsymbol{\varepsilon}$  : the vector of random measurement errors and assumed to be zero mean and uncorrelated with constant variance.

The Ordinary Least Square (OLS) identification method is based on the Equation Error Method. According to this, the identification of parameter vector  $\theta$  is equivalent to the minimization of a scalar cost function [8, 22]:

$$\mathbf{J}(\theta) = \frac{1}{2} \mathbf{a}^T \boldsymbol{\varepsilon}^2 = \frac{1}{2} \mathbf{a}^T (\mathbf{z} - \mathbf{H}\theta)^2 \quad (13)$$

Solving equation  $\frac{\partial \mathbf{J}}{\partial \theta} = 0$  for the unknown parameter vector  $\theta$  gives the formula for the OLS estimator:

$$\hat{\theta} = (\mathbf{H}^T \mathbf{H})^{-1} \mathbf{H}^T \mathbf{z} \quad (14)$$

In practical cases, the assumptions of uncorrelated measurement errors and homogeneous variance are not valid [22]. The noise covariance matrix  $\mathbf{V}$  is

introduced and the formula for Weighted Least Squares (WLS) estimator:

$$\hat{\theta} = (\mathbf{H}^T \mathbf{V}^{-1} \mathbf{H})^{-1} \mathbf{H}^T \mathbf{V}^{-1} \mathbf{z} \quad (15)$$

To validate the result of estimator, the Mean Squares Error (MSE)  $s^2$  can be estimated [22]:

$$s^2 = \frac{1}{N} \sum_{i=1}^N \hat{z}(i) - z(i) \quad (16)$$

#### 4. Experiments and data processing

Trials with *Gavia* AUV were conducted on May 13, 2015 at Trevallyn Lake, Tasmania, Australia in relatively calm wind and current conditions. Free running tests for both longitudinal and lateral subsystem identifications were performed separately to fully excite the dynamic models of AUV system. It is important to design the missions that covers the total operational range. For experiments in the vertical plane, the AUV was continuously changing depth in the range of 0- 5 m while maintaining constant heading. Experiments in the horizontal plane were controlled by performing turning manoeuvres at constant depth. The control surface angles varied from - 20 to 20 deg. During all experiments, the vehicle was commanded to track predefined waypoints with a constant forward speed at 1.6 m/s .

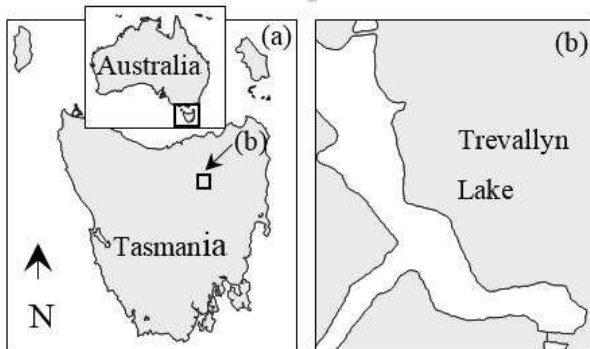


Fig. 5. Experimental site is located at (b) Trevallyn Lake near (a) Launceston city, Tasmania, Australia

The *Gavia* AUV was instrumented to measure the necessary state variables. It used the Kearfott T-24 integrated seaborne navigation system combined with a Kalman filter. The INS provided accurate linear and

angular accelerations, the Doppler Velocity Log (DVL) provided velocity [24]. In previous works, the acceleration data were usually obtained by numerical differentiation of gyro data due to lack of the efficient acceleration sensors [12, 13]. With direct measurements of acceleration data in this study, the errors resulted from differentiation process could be neglected. In addition, the 3DM-GX1 Gyro Enhanced Orientation Sensor supplied additional information about the angular velocity and orientation. Since there are no integrated sensors to measure the actual control surface angles, the commanded angles sent by the autopilot system were used.

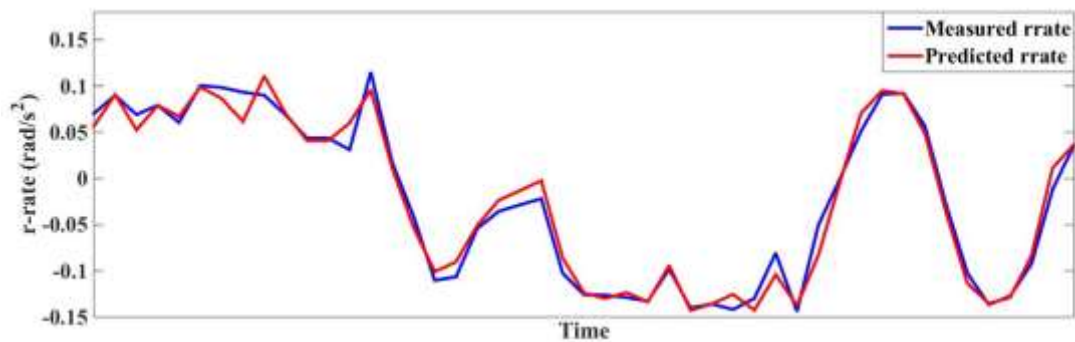
The measured trial dynamic data obtained by the on-board sensors were filtered and stored. Prior to applying in identification procedure, these data from were resampled to form an integrated set of data since the sensors had different sampling rates. The final sampling rate for the integrated set of data is 0.5 Hz .

#### 5. Results and Discussion

After pre-processing data from system files, previously described methods were applied to identify the model parameters for both lateral and longitudinal subsystems. The initial goal is to fit the experimental measured angular acceleration data to predicted data and then the final objective is to optimise the identified model by fitting the experimental data to simulated data generating from numerical simulator. Four segments of data were used in this stage for lateral and longitudinal subsystem identification respectively.

Fig. 6 and Fig. 7 illustrate the comparison of predicted results of angular acceleration and measured results. As can be seen, the data from predicted models are in general in good fit with the experimental measured data. The mean square errors are  $s_1^2 = 1.92 \cdot 10^{-4}$  for  $\delta$  (r-rate) data and  $s_2^2 = 1.94 \cdot 10^{-4}$  for  $\phi$  (q-rate) data. The residual calculations are also performed to examine the fitness between measured and predicted data. There are overshoots and undershoots at some points. This might be a consequence of fast response of physical system in which angular velocity and acceleration could not be captured accurately by sensors. In addition, angular velocity and acceleration data were recorded by two sensors separately (Gyro and INS).

(a)



(b)

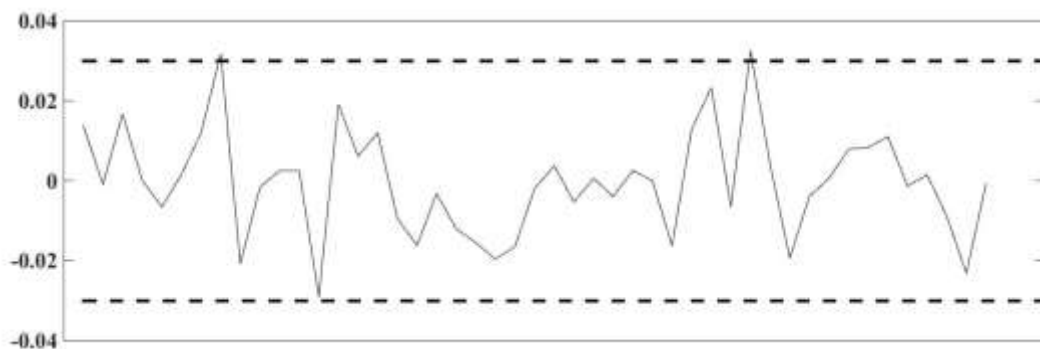
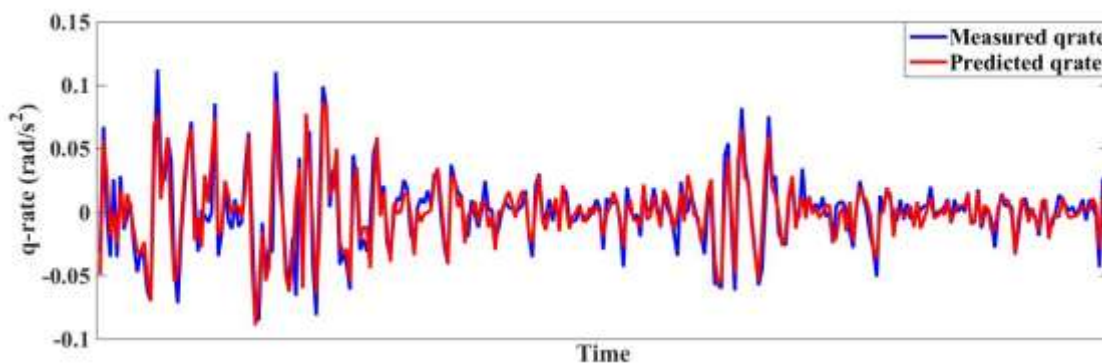


Fig. 6. (a) Comparison between the predicted (red lines) and measured (blue lines) angular accelerations for lateral subsystem and (b) the residuals

(a)



(b)

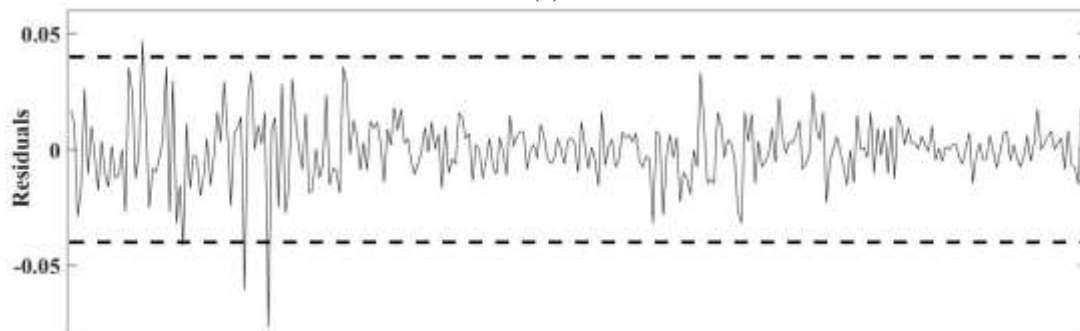


Fig. 7. (a) Comparison between the predicted (red lines) and measured (blue lines) angular accelerations for the longitudinal subsystem and (b) the residuals

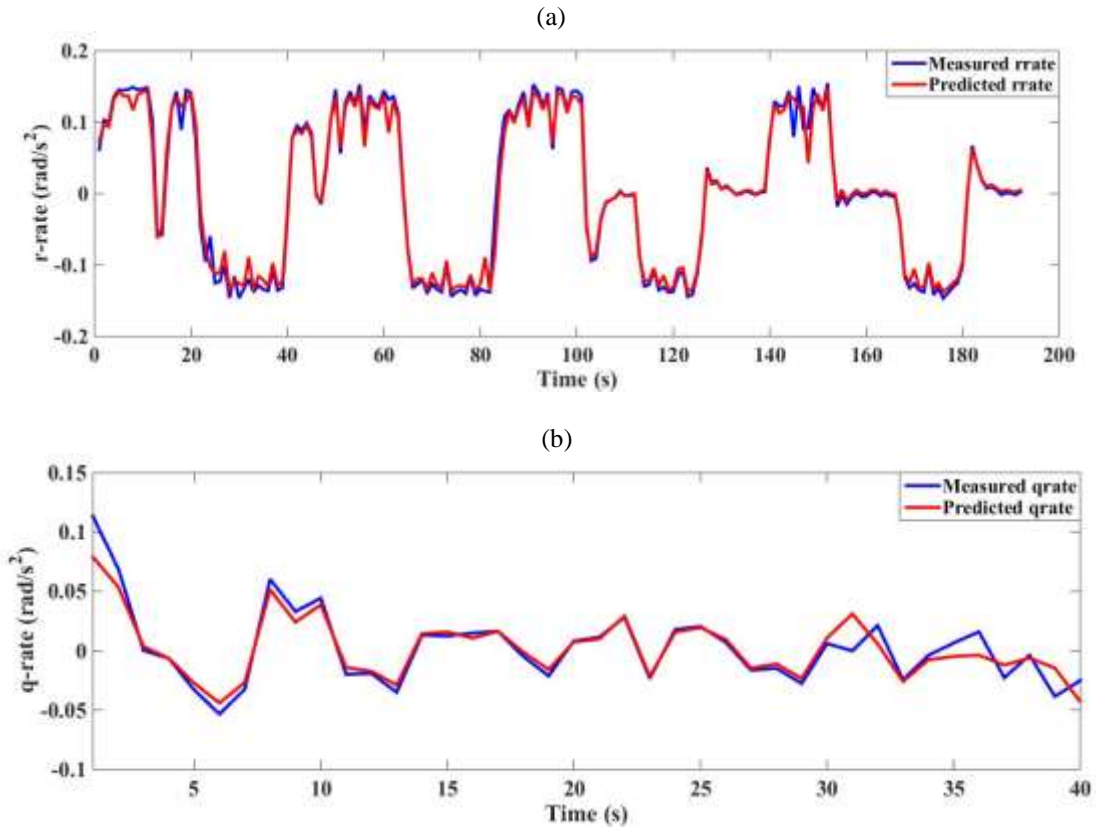


Fig. 8. Comparison between the predicted (red lines) and measured (blue lines) angular accelerations for (a) the lateral subsystem and (b) the longitudinal subsystems

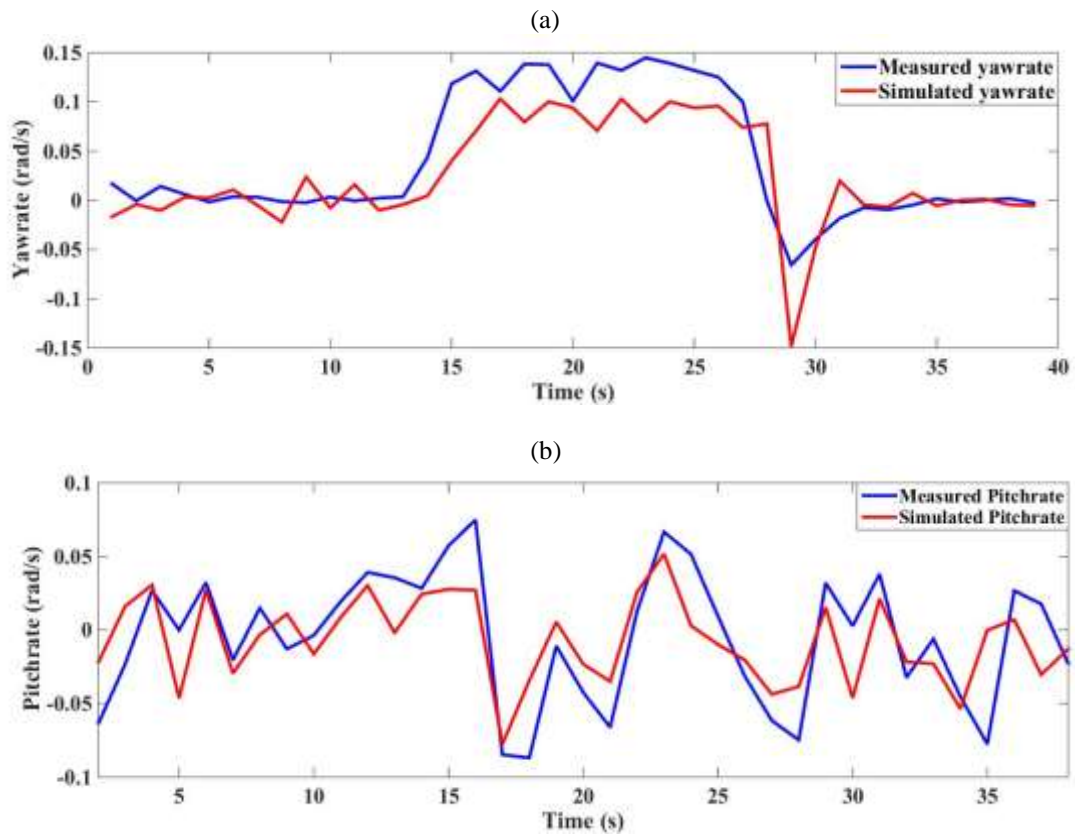


Fig. 9. Comparison between the simulated (red lines) and measured (blue lines) angular accelerations resulted from optimisation procedure for (a) the lateral subsystem and (b) the longitudinal subsystem

Another set of experimental data, different from the data used to construct the mathematical model, is applied to verify the fidelity of estimated parameter. From the result shown in Fig. 8, it can be concluded that the identified model are able to predict the system response from given state's values.

From the identified model, a simulator is proposed with the attempt to accurately simulate the model from specified initial condition. This initial conditions are selected as the first state values in the set of experimental data used for simulation validation. In Fig. 9, numerical simulation results of optimised model for angular acceleration are compared to the actual measured results for a set of experimental data. The responses from the simulation program demonstrate a good agreement with the measured data.

The parameters obtained from the LS optimised model are summarised in Table 2. It is worth noting that the absolute values of four control surface hydrodynamic parameters  $b_i$  and  $d_i$  are identical in each subsystem. The sign difference is resulted from the definition of rotational direction for each control surface. In addition, from the obtained values of the parameters  $a_1, c_1, c_2$ , the stability of yaw and pitch dynamics are able to be analysed based on the stability conditions of linear state space model.

From equation (5) the eigenvalues of the matrix  $A = \begin{bmatrix} \dot{\phi}_1 & 0 & \dot{\phi} & 0 \\ \dot{\phi} & 1 & 0 & 0 \\ \dot{\phi} & 0 & \dot{\phi} & 1 \\ \dot{\phi} & 0 & \dot{\phi} & 0 \end{bmatrix}$  are  $l_{A1} = -0.9497$  and  $l_{A2} = 0$ . Since  $l_{A1} \neq 0$  and  $l_{A2} \neq 0$  the yaw dynamic of AUV is stable.

From equation (6) the eigenvalues of the matrix  $B = \begin{bmatrix} \dot{\phi}_1 & c_2 & 0 & \dot{\phi} & 0.9093 & -0.0094 & 0 \\ \dot{\phi} & 1 & 0 & 0 & 0 & 0 & 0 \\ \dot{\phi} & 0 & 0 & \dot{\phi} & 1 & 0 & 0 \\ \dot{\phi} & 0 & -U_0 & 0 & 0 & -1.6 & 0 \end{bmatrix}$  are  $l_{B1} = 0$ ,  $l_{B2} = -0.0105$  and  $l_{B3} = -0.8988$ . Since  $l_{B1}, l_{B2}, l_{B3} \neq 0$  the pitch dynamic of AUV is stable.

Table 2. Identified parameters for longitudinal and diving subsystems

Lateral Subsystem		Longitudinal Subsystem	
Parameter	Value	Parameter	Value
$a_1$	-0.9497	$c_1$	-0.9093
$b_1$	0.00062	$c_2$	-0.0094
$b_2$	-0.00062	$d_1$	-0.006
$b_3$	0.00062	$d_2$	0.006
$b_4$	-0.00062	$d_3$	0.006
		$d_4$	-0.006

### 6. Conclusions and future works

In this study, the simulator describing the manoeuvring characteristics of torpedo-shaped

underwater vehicle in the vertical and horizontal planes has been developed. Using collected trial data, model parameters are identified using a LS approach. The simulator is feasible to simulate the longitudinal and lateral subsystems starting from specified initial conditions. The obtained results have proved the effectiveness of Least Squares method in system identification of hydrodynamic coefficients of a torpedo-shaped underwater vehicle. For future work, this study provides a good foundation for further developing simulation study and facilitate the advance control design of autonomous underwater vehicle equipped with new developed propulsion system.

### References

- [1] G. N. Roberts and R. Sutton, *Advances in unmanned marine vehicles* vol. 69: Iet, 2006.
- [2] G. N. Roberts and R. Sutton, *Further advances in unmanned marine vehicles* vol. 77: IET, 2012.
- [3] T. Prestero, "Development of a six-degree of freedom simulation model for the REMUS autonomous underwater vehicle," in *OCEANS, 2001. MTS/IEEE Conference and Exhibition, 2001*, pp. 450-455.
- [4] P. Ridao, J. Battle, and M. Carreras, "Model identification of a low-speed UUV," in *IFAC Conference Control Applications in Marine Systems, Glasgow, Scotland, 2001*.
- [5] A. Phillips, M. Furlong, and S. R. Turnock, "The use of computational fluid dynamics to assess the hull resistance of concept autonomous underwater vehicles," in *OCEANS 2007-Europe, 2007*, pp. 1-6.
- [6] S. A. T. Randeni. P., Z. Q. Leong, D. Ranmuthugala, A. L. Forrest, and J. Duffy, "Numerical investigation of the hydrodynamic interaction between two underwater bodies in relative motion," *Applied Ocean Research*, June 2015, vol. 51, pp. 14-24, 2015.
- [7] J. P. Avila, D. C. Donha, and J. C. Adamowski, "Experimental model identification of open-frame underwater vehicles," *Ocean Engineering*, vol. 60, pp. 81-94, 2013.
- [8] L. Ljung, *System identification*: Springer, 1998.
- [9] S. C. Martin and L. L. Whitcomb, "Experimental identification of six-degree-of-freedom coupled dynamic plant models for underwater robot vehicles," *Oceanic Engineering, IEEE Journal of*, vol. 39, pp. 662-671, 2014.
- [10] J. D. Weiss and N. E. Du Toit, "Real-time dynamic model learning and adaptation for underwater vehicles," in *Oceans-San Diego, 2013, 2013*, pp. 1-10.
- [11] K. M. Fauske, F. Gustafsson, and O. Hegrenæs, "Estimation of AUV dynamics for sensor fusion," in *Information Fusion, 2007 10th International Conference on*, 2007, pp. 1-6.

- [12] E. Y. Hong, T. K. Meng, and M. Chitre, "Online system identification of the dynamics of an Autonomous Underwater vehicle," in *Underwater Technology Symposium (UT), 2013 IEEE International*, 2013, pp. 1-10.
- [13] J. Petrich, W. L. Neu, and D. J. Stilwell, "Identification of a simplified AUV pitch axis model for control design: Theory and experiments," in *OCEANS 2007*, 2007, pp. 1-7.
- [14] *GAVIA Autonomous Underwater Vehicle User Manual*: Teledyne GAVIA ehf., 2012.
- [15] T. I. Fossen, *Handbook of marine craft hydrodynamics and motion control*: John Wiley & Sons, 2011.
- [16] N. V. Hoffer, C. Coopmans, A. M. Jensen, and Y. Chen, "A survey and categorization of small low-cost unmanned aerial vehicle system identification," *Journal of Intelligent & Robotic Systems*, vol. 74, pp. 129-145, 2014.
- [17] A. Tiano, "Comparison of non linear identification methods for underwater vehicles," in *Control, Communications and Signal Processing, 2004. First International Symposium on*, 2004, pp. 549-552.
- [18] T. Fossen, "Marine Control Systems: Guidance, Navigation and Control of Ships, Rigs and Underwater Vehicles. Marine Cybernetics, Trondheim, Norway, 2002," ISBN 82-92356-00-2.
- [19] A. Tiano, R. Sutton, A. Lozowicki, and W. Naeem, "Observer Kalman filter identification of an autonomous underwater vehicle," *Control engineering practice*, vol. 15, pp. 727-739, 2007.
- [20] M. Caccia, G. Indiveri, and G. Veruggio, "Modeling and identification of open-frame variable configuration unmanned underwater vehicles," *Oceanic Engineering, IEEE Journal of*, vol. 25, pp. 227-240, 2000.
- [21] B. Jalving, "The NDRE-AUV flight control system," *Oceanic Engineering, IEEE Journal of*, vol. 19, pp. 497-501, 1994.
- [22] V. Klein and E. A. Morelli, *Aircraft system identification: theory and practice*: American Institute of Aeronautics and Astronautics Reston, VA, USA, 2006.
- [23] P. Chirarattananon and R. J. Wood, "Identification of flight aerodynamics for flapping-wing microrobots," in *Robotics and Automation (ICRA), 2013 IEEE International Conference on*, 2013, pp. 1389-1396.
- [24] T. Hiller, T. Reed, and A. Steingrimsson, "Producing Chart Data from Interferometric Sonars on Small AUVs," *The International Hydrographic Review*, 2011.

## Biography



**Mr Minh Quang Tran** is currently a PhD student at the Australian Maritime College, University of Tasmania. He obtained his Bachelor of Engineering in Aerospace Engineering from University of Technology at Vietnam National University in 2014. His research

interests are underwater vehicle's propulsion system, simulation and control of marine vehicles.



**Mr Supun Randeni** is currently a PhD candidate at the Australian Maritime College of University of Tasmania. He obtained his Bachelor of Engineering Honours degree in Naval Architecture from the same university in 2013. His main

research interests are in the fields of hydrodynamics, underwater vehicles and autonomous systems. Upon the completion of the PhD, he will continue to establish himself in the maritime research industry.



**Dr Hung Duc Nguyen** is a lecturer and Graduate Research Coordinator at National Centre for Maritime Engineering and Hydrodynamics, Australian Maritime College, University of Tasmania. He obtained his Ph.D. degree from Tokyo University of Marine Science and

Technology, Japan. His research interests are Guidance, Navigation and Control of Marine Vehicles and Offshore Structures; Ship Manoeuvring Dynamics and Manoeuvrability; GPS/GNSS and Inertial Navigation Systems; Linear and Non-Linear Control Systems; Modelling and Recursive/Stochastic Estimation of Marine and Offshore Control Systems; Fault Detection and Monitoring Based on Modelling and Estimation; Instrumentation and Process Control; Sea-Keeping and Roll Stabilization Systems; Marine Robots and Control Applications in Underwater Vehicles.



**Associate Professor Jonathan Binns** is a director, ARC Research Training Centre for Naval Design and Manufacturing and Associate Dean Research at Australian Maritime College, University of Tasmania. He

obtained his Ph.D. degree from Australian Maritime College, Australia. His research interests are applied hydrodynamics, design and analysis of sailing yachts, sailing simulation, design and analysis of naval platforms, design and analysis of offshore structures.



**Dr Alexander Forrest** is a lecturer and the course coordinator of Ocean Engineering at Australian Maritime College, University of Tasmania and a researcher at University of California – Davis. He obtained his Ph.D. degree from University of British

Columbia, Canada. His current research area of interest is the use of Autonomous Underwater Vehicles (AUVs) as data collection platforms for examining water column hydrodynamics and benthic habitat mapping (using both image and acoustic techniques). Specifically he uses innovative engineering techniques to conduct novel science experiments in often times challenging (i.e., under-ice) environments.



**Dr Shuhong Chai** is a director of National Centre for Maritime Engineering and Hydrodynamics at Australian Maritime College, University of Tasmania. She obtained her Ph.D. degree from

Universities of Glasgow and Strathclyde, Glasgow, UK. Her research interests are Hydrodynamics of Offshore Structures, Fluid-Structure Interaction, Vortex-Induced Vibration, Deep water Marine Risers, Mooring lines, and Subsea Pipelines, Wave Mechanics, Coastal Engineering, Near shore Hydrodynamics.